24th COBEM - 2017

24th ABCM International Congress of Mechanical Engineering
December 3-8, 2017, Curitiba, PR, Brazil

COBEM-2017-0393
Ultrasound reflection from immersed laminates and its application in adhesive bond inspections

Bernardo Junqueira
Daniel Castello
Department of Mechanical Engineering, Poli/COPPE, Universidade Federal do Rio de Janeiro (UFRJ), Rio de Janeiro, RJ, Brazil
bernardofeijo@id.uff.br, castello@mecanica.ufrj.br

Ricardo Leiderman
Computer Science Department, Universidade Federal Fluminense (UFF), Av. Gal. Milton Tavares de Souza, s/nº, São Domingos, Niterói, RJ, 24210-346, Brazil
leider@ic.uff.br

Arthur M. B. Braga
Department of Mechanical Engineering, Pontífica Universidade Católica do Rio de Janeiro (PUC-Rio), Rua Marquês de São Vicente, 225, Gávea, Rio de Janeiro, RJ, 22453-900, Brazil
abraga@puc-rio.br

Abstract. *In the present work, we compute the reflection coefficient for immersed laminated plates. We use the spring boundary conditions for adhesive bonds and model adhesion imperfections reducing the corresponding spring constants. We develop our formulation with the aid of the invariant embedding technique and, accordingly, it is numerically unconditionally stable. We identify the frequencies/angles of incidence that are most sensitive to adhesion flaws. Such frequencies/angles of incidence are presumably the optimum choices for the inspecting field in adhesive bond ultrasound evaluations.*

Keywords: *Interface inspection, Laminates, Spring boundary conditions, Invariant embedding.*

1. INTRODUCTION

The focus of the present work is in the ultrasonic inspection of adhesive bonds. In many cases, degradation of the thin adhesive layer, rather than of the bulk of the adherents, leads to catastrophic failure. The implementation of a reliable non destructive evaluation to attest the integrity of such a difficult-to-access region is still an open task.

2. GOVERNING EQUATIONS

2.1 Elastic Layers

It is assumed that the wave fields are time harmonic and, therefore, satisfy the following equations for stress $\boldsymbol{\sigma}$ and displacement $\boldsymbol{u}$ in solid layers:

$$\nabla\boldsymbol{\sigma} + \rho\omega^2\boldsymbol{u} = 0 \tag{1}$$

$$\boldsymbol{\sigma} = \boldsymbol{C} : \boldsymbol{\varepsilon} \tag{2}$$

$$\boldsymbol{\varepsilon} = \frac{1}{2}(\nabla\boldsymbol{u} + \nabla\boldsymbol{u}^T) \tag{3}$$

where $\boldsymbol{C}$ is the elasticity tensor, $\boldsymbol{\varepsilon}$ is the strain tensor for small deformations, ρ is the density and ω is the angular frequency. $\boldsymbol{C}$ and ρ may vary from layer to layer. This formulation is made with the aid of the invariant embedding

technique (Bellman and Kalaba, 1959). Accordingly, the displacement $\boldsymbol{u}$ and traction $\boldsymbol{t}$ were decomposed into upgoing and downgoing fields:

$$\boldsymbol{u} = \boldsymbol{u}_1 + \boldsymbol{u}_2 \tag{4}$$

$$\boldsymbol{t} = \boldsymbol{t}_1 + \boldsymbol{t}_2 \tag{5}$$

where the subscript 1 is associated to upgoing fields, positive vertical (z) direction, while the subscript 2 is associated to downgoing fields, negative vertical (z) direction.

From the exact solution of the elastodynamic equations of motion, the $3x3$ matrix operators $\boldsymbol{M_1}(z)$, $\boldsymbol{M_2}(z)$, $\boldsymbol{Z_1}$ and $\boldsymbol{Z_2}$ are determined. The operators $\boldsymbol{M_1}(z)$ and $\boldsymbol{M_2}(z)$ propagate the up and downgoing displacement fields within each layer:

$$\bar{\boldsymbol{u}}_{\boldsymbol{j}}(z_2) = \boldsymbol{M_j}(z_2 - z_1)\bar{\boldsymbol{u}}_{\boldsymbol{j}}(z_1), j = 1, 2 \tag{6}$$

While the local impedance tensors $\boldsymbol{Z_1}$ and $\boldsymbol{Z_2}$, in turn, relate the up and downgoing traction vectors to the respective displacement fields:

$$\bar{\boldsymbol{t}}_{\boldsymbol{j}}(z_2) = -i\omega \boldsymbol{Z_j}\bar{\boldsymbol{u}}_{\boldsymbol{j}}, j = 1, 2 \tag{7}$$

where z_1 and z_2 are the $z - axis$ coordenates of the beggining and the end of a layer, respectively. Further details and the definitions for $\boldsymbol{M_j}(z)$ and $\boldsymbol{Z_j}$ for isotropic medium can be found in Leiderman *et al.* (2005, 2007).

2.2 Adhesive Layers

The thin adhesive layer was treated as infinitesimally thick and replaced by a set of equivalent tangential and normal springs. This approach is known as the Quasi Static Approximation (QSA) and was apparently first proposed by Baik and Thompson (1984). This assumption is valid when the inspecting wavelength is much larger than the interfacial layer thickness and it gives us the following spring boundary conditions:

$$\boldsymbol{K}[\boldsymbol{u}^+ - \boldsymbol{u}^-] = \boldsymbol{t}^+ \tag{8}$$

$$\boldsymbol{t}^- = \boldsymbol{t}^+ \tag{9}$$

In the Eq. (8) and (9) the superscript " $+$ " indicates the values of the field variables immediately above the interface, while the superscript " $-$ " indicates those immediately below. $\boldsymbol{K}$ is a $3x3$ diagonal spring matrix where the precise values of normal and tangencial constants can be written in terms of elastic properties and nominal thickness of the interfacial layer (Rokhlin and Huang, 1992):

$$\boldsymbol{K} = \left(h_{interface} \times \begin{bmatrix} s_{int} & 0 & 0 \\ 0 & s_{int} & 0 \\ 0 & 0 & 1/c_{int} \end{bmatrix} \right)^{-1} \tag{10}$$

$$s_{int} = \frac{1}{\mu_{interface}} \tag{11}$$

$$c_{int} = 2 * \mu_{interface} + \lambda_{interface} \tag{12}$$

Since its introduction, the QSA has been extensively used in theoretical works to model adhesive bonds and rough contact interfaces between solids (Golub, 2010; Golub and Boström, 2011; Rokhlin and Huang, 1992; Rajabi and Hashemi-nejad, 2009; Pialucha and Cawley, 1992; Li *et al.*, 1992).

Higher order extension of similar model for thin layer has been recently described in Zakharov (2006) and An *et al.* (2013). In the context of the QSA, defective bonds are usually modeled by a reduction in the spring constants (Angel and Achenbach, 1984).

3. COMPUTATIONAL PROCEDURE

In this section a recursive algorithm is presented to compute the reflection coefficient at the top of a laminate immersed in acoustic fluid. To that end, it is desired to work with the surface impedance tensors of the solid. More specifically, the layered structure is swept in a bottom up fashion, computing the surface impedance tensor $\boldsymbol{G}$ presented in each layer, as schematically depicted in Fig. 1.

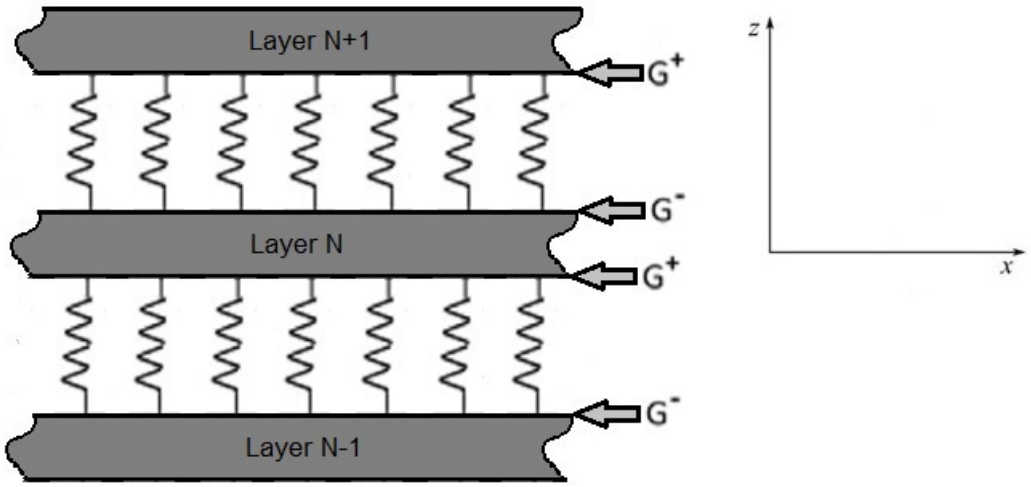

Figure 1. Surface impedance tensor calculation scheme, where G^+ is the impedance tensor immediately above the interface and G^- immediately bellow

The surface impedance tensor is defined through the relation:

$$\bar{\boldsymbol{t}} = -i\omega \boldsymbol{G} \bar{\boldsymbol{u}} \tag{13}$$

In the sense of what is said above, the first step consists of the computation of the surface impedance at the bottom of the laminate. For an acoustic fluid half-space in which the radiation condition is satisfied at infinity, $\boldsymbol{G} = \boldsymbol{Z_f}$, where $\boldsymbol{Z_f}$ is the fluid local impedance tensor:

$$\boldsymbol{Z_f} = \begin{bmatrix} 0 & 0 & 0 \\ 0 & 0 & 0 \\ 0 & 0 & Z_f \end{bmatrix} \tag{14}$$

$$Z_f = \frac{\rho_f \omega}{\gamma} \tag{15}$$

Since ρ_f is the fluid density and γ is the fluid wave number in the z (vertical) direction.

At this point, the reflection matrix $\boldsymbol{R}$ that relates the downgoing to the upgoing displacement at the first layer's bottom is introduced, so that:

$$\bar{\boldsymbol{u}}_{\boldsymbol{1}} = \boldsymbol{R} \bar{\boldsymbol{u}}_{\boldsymbol{2}} \tag{16}$$

solving for $\boldsymbol{R}$ we get:

$$\boldsymbol{R} = (\boldsymbol{G} - \boldsymbol{Z_1})^{-1} (\boldsymbol{Z_2} - \boldsymbol{G}) \tag{17}$$

where $\boldsymbol{Z_1}$ and $\boldsymbol{Z_2}$ are the up and downgoing local impedance tensors associated to the solid, respectively.

In the next step, the surface impedance tensor at the top of the first elastic layer is computed:

$$\boldsymbol{G} = [\boldsymbol{Z_1 M_1}(h_1)\boldsymbol{R M_2}(-h_1) + \boldsymbol{Z_2}][\boldsymbol{M_1}(h_1)\boldsymbol{R M_2}(-h_1) + \boldsymbol{I}]^{-1} \tag{18}$$

where h_1 is the layer thickness.

To represent the thin adhesive layer it is considered an infinitesimally thick distribution of normal and tangential springs on the top of the first layer. In that sense, the Eqs. (8) and (9) are used to compute:

$$\boldsymbol{G}^+ = (\boldsymbol{I} - i\omega \boldsymbol{G K}^{-1})^{-1}\boldsymbol{G} \tag{19}$$

where $\boldsymbol{I}$ is the identity matrix and $\boldsymbol{K}$ is the spring matrix associated to the interfacial adhesive layer. $\boldsymbol{G}^+$ is the surface impedance presented in the second elastic layer.

Equations (17) – (19) can be used recursively to determine the surface impedance presented to the upper fluid half-space. Then, this can be used to compute the reflection at the laminate's top. First, we define the reflection coefficient as:

$$r = \frac{\bar{w}_1}{\bar{w}_2} \tag{20}$$

where $\bar{w}_2$ is the normal component of the incident displacement field, while $\bar{w}_1$ is the normal component of the reflected displacement field. Since there are only P-waves propagating in the fluid half-space, the other in-plane component of the displacement field can be computed from the normal one, if desired. The classic boundary conditions at the solid/fluid interface are:

$$\boldsymbol{t}^- = \boldsymbol{t}^+ = -\bar{p}\boldsymbol{n} \tag{21}$$

$$\bar{w}^+ = \bar{w}^- \tag{22}$$

where $\bar{p}$ is the pressure in the fluid that can be computed as $\bar{p} = -i\omega Z_f(\bar{w}_2^+ - \bar{w}_1^+)$ and $\boldsymbol{n}$ is the outward unit vector in the z direction. From the equations above, the following relation can be written:

$$[\boldsymbol{G} + \boldsymbol{Z_f}]\bar{\boldsymbol{u}}^- = \begin{bmatrix} 0 & 0 & 2Z_f\bar{w}_2^+ \end{bmatrix}^T \tag{23}$$

Recall that $\boldsymbol{Z_f}$ and Z_f were previously defined in the beginning of this section. r can then be straightforwardly computed as $r = \bar{w}^- - 1$ by solving Eq. (23) with $\bar{w}_2^+ = 1$.

4. RESULTS AND DISCUSSION

We illustrate the application of the proposed methodology computing the reflection coefficient of a three-layer plate immersed in water. The plate is made of a stainless steel layer with $2cm$ thickness, an aluminium layer with $3cm$ thickness, and a copper layer with $10cm$ thickness (from the bottom up). In addition, there is an epoxy layer with $100\mu m$ nominal thickness between each pair of constituent layers, acting as adhesive. We give in Tab. 1 the wave speeds and density for each constituent layer, as well as for the epoxy.

Table 1. Mechanical properties of constituent materials.

Material	Density (kg/m^3)	P-wave speed (m/s)	S-wave speed (m/s)
Aluminium	2700	6320	3130
Copper	8930	4660	2160
Epoxy	1200	2150	1030
Stainless Steel	7750	5564	3120
Water	1000	1480	0

Figure 2 shows the reflection coefficient as function of the angle of incidence for $102.8kHz$. The continuous line is related the flawless laminated plate, while the dashed line is related to a reduced interfacial stiffness xx component of the

interface between the stainless steel and aluminum layers. We reduced the interfacial stiffness's xx component in order to model a kissing bond. The figure shows that 4.1^{o} would be a good choice for the angle of incidence.

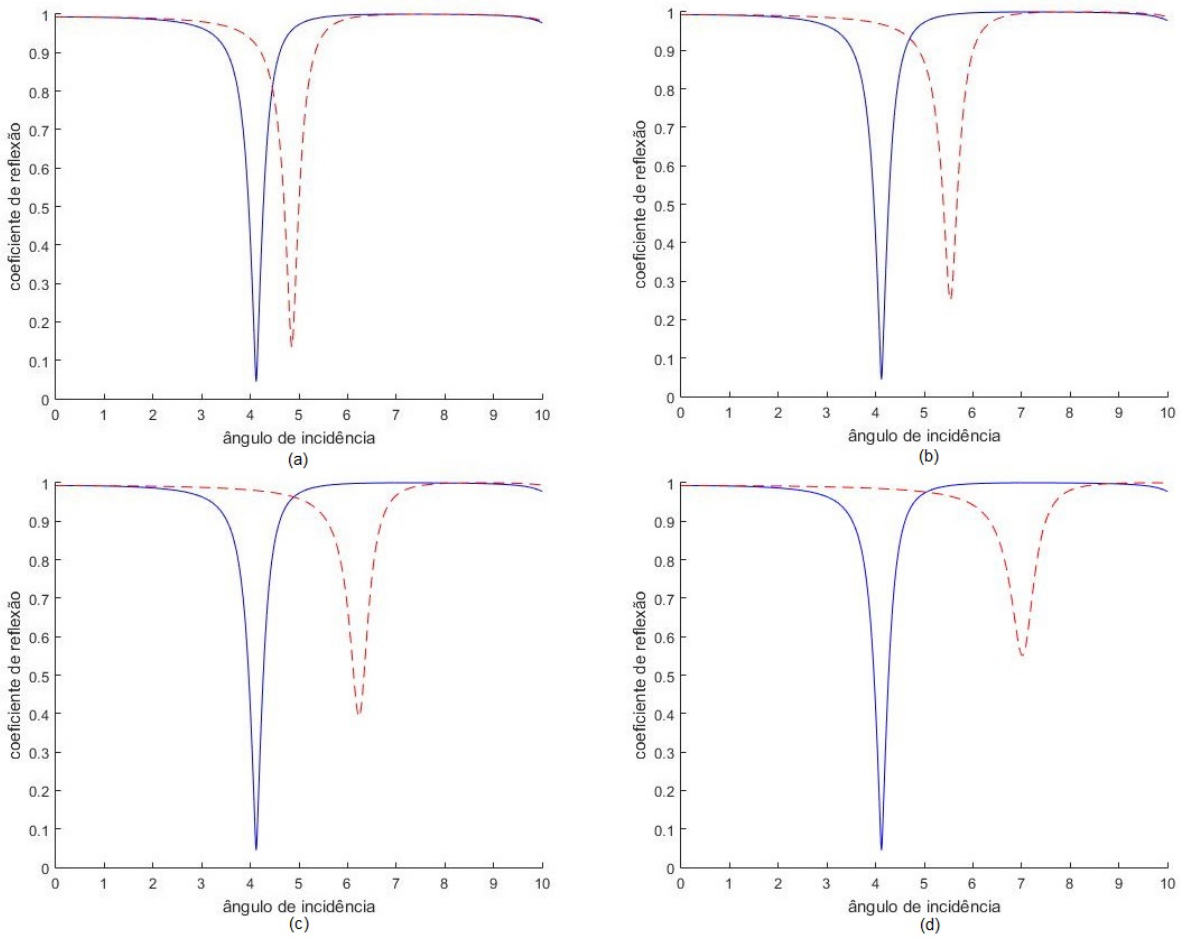

Figure 2. Reflection coefficient as function of the angle of incidence for defect in the first adhesive layer. (a) 80% of original stiffness. (b) 60% of original stiffness. (c) 40% of original stiffness. (d) 20% of original stiffness.

Figure 3 shows the reflection coefficient as function of the angle of incidence for $96.5kHz$. Analogously to Fig. 2, the continuous line is related the flawless laminated plate, while the dashed line is related to a reduced interfacial stiffness xx component of the interface between the aluminium and copper layers. The figure shows that 9^{o} would be a good choice for the angle of incidence.

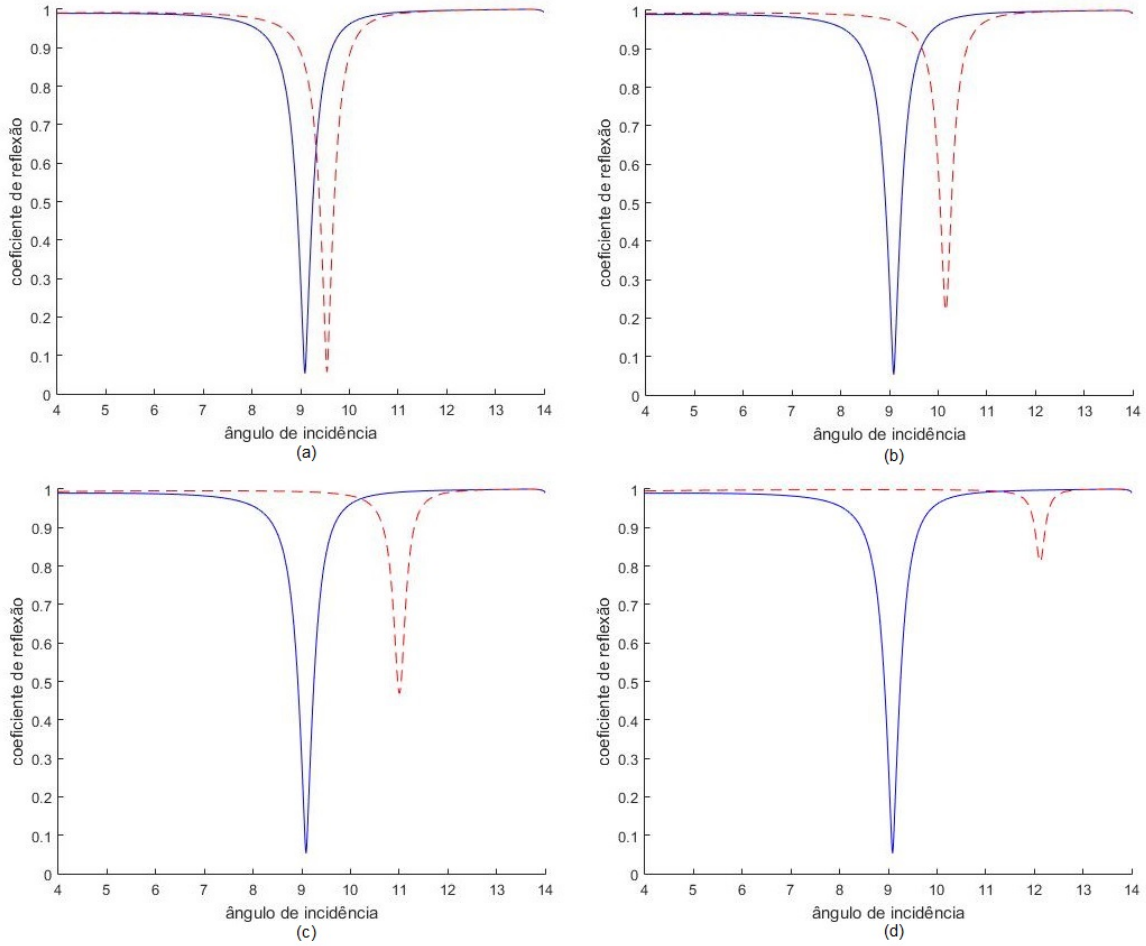

Figure 3. Reflection coefficient as function of the angle of incidence for defect in the second adhesive layer. (a) 80% of original stiffness. (b) 60% of original stiffness. (c) 40% of original stiffness. (d) 20% of original stiffness.

5. CONCLUSIONS

In the present work, we computed the reflection coefficient for an adhesively bonded three-layer plate immersed in water. In addition, we identified the frequencies/angles of incidence that are most sensitive to adhesion flaws. Those are presumably the optimum choices for the inspecting field in adhesive bond ultrasound evaluations.

6. ACKNOWLEDGEMENTS

The authors acknowledge the support of the Brazilian research agencies CNPq and CAPES.

7. REFERENCES

An, Z., Wang, X., Deng, M., Mao, J. and Li, M., 2013. "A nonlinear spring model for an interface between two solids". *Wave Motion*, Vol. 50, No. 2, pp. 295 – 309. ISSN 0165-2125. doi:https://doi.org/10.1016/j.wavemoti.2012.09.004. URL `http://www.sciencedirect.com/science/article/pii/S0165212512001278`.

Angel, Y.C. and Achenbach, J.D., 1984. "Reflection and transmission of elastic waves by a periodic array of cracks". *Journal of Applied Mechanics*, Vol. 52, pp. 33–41.

Baik, J.M. and Thompson, R.B., 1984. "Ultrasonic scattering from imperfect interfaces: A quasi-static model". *Journal of Nondestructive Evaluation*, Vol. 4, No. 3, pp. 177–196. ISSN 1573-4862. doi:10.1007/BF00566223. URL `http://dx.doi.org/10.1007/BF00566223`.

Bellman, R. and Kalaba, R., 1959. "Functional equations, wave propagation, and invariant imbedding". *J. Math. Mech.*, Vol. 8, p. 683.

Golub, M.V., 2010. "Propagation of elastic waves in layered composites with microdefect concentration zones and their simulation with spring boundary conditions". *Acoustical Physics*, Vol. 56, No. 6, pp. 848–855. ISSN 1562-6865.

doi:10.1134/S1063771010060084. URL http://dx.doi.org/10.1134/S1063771010060084.

Golub, M.V. and Boström, A., 2011. "Interface damage modeled by spring boundary conditions for in-plane elastic waves". *Wave Motion*, Vol. 48, No. 2, pp. 105 – 115. ISSN 0165-2125. doi:https://doi.org/10.1016/j.wavemoti.2010.09.003. URL http://www.sciencedirect.com/science/article/pii/S0165212510000818.

Leiderman, R., Barbone, P.E. and Braga, A.M.B., 2007. "Reconstructing the adhesion stiffness distribution in a laminated elastic plate: Exact and approximate inverse scattering solutions". *The Journal of the Acoustical Society of America*, Vol. 122, No. 4, pp. 1906–1916. doi:10.1121/1.2772212. URL http://dx.doi.org/10.1121/1.2772212.

Leiderman, R., Braga, A.M.B. and Barbone, P.E., 2005. "Scattering of ultrasonic waves by defective adhesion interfaces in submerged laminated plates". *The Journal of the Acoustical Society of America*, Vol. 118, No. 4, pp. 2154–2166. doi:10.1121/1.2036147. URL http://dx.doi.org/10.1121/1.2036147.

Li, B., Hefetz, M. and Rokhlin, S.I., 1992. "Ultrasonic evaluation of environmentally degraded adhesive joints". *Rev. Prog. Quant. Nondestr. Eval.*, Vol. 11, pp. 1221–1228.

Pialucha, T. and Cawley, P., 1992. "The detection of a weak adhesive/adherend interface in bonded joints by ultrasonic reflection measurements". *Rev. Prog. Quant. Nondestr. Eval.*, Vol. 11, pp. 1261–1266.

Rajabi, M. and Hasheminejad, S.M., 2009. "Acoustic resonance scattering from a multilayered cylindrical shell with imperfect bonding". *Ultrasonics*, Vol. 49, No. 8, pp. 682 – 695. ISSN 0041-624X. doi:https://doi.org/10.1016/j.ultras.2009.05.007. URL http://www.sciencedirect.com/science/article/pii/S0041624X09000626.

Rokhlin, S.I. and Huang, W., 1992. "Ultrasonic wave interaction with a thin anisotropic layer between two anisotropic solids: Exact and asymptotic-boundary-condition methods". *The Journal of the Acoustical Society of America*, Vol. 92, No. 3, pp. 1729–1742. doi:10.1121/1.403912. URL http://dx.doi.org/10.1121/1.403912.

Zakharov, D.D., 2006. "High order approximate low frequency theory of elastic anisotropic lining and coating". *The Journal of the Acoustical Society of America*, Vol. 119, No. 4, pp. 1961–1970. doi:10.1121/1.2169922. URL http://dx.doi.org/10.1121/1.2169922.

8. RESPONSIBILITY NOTICE

The authors are the only responsible for the printed material included in this paper.